Journal of Power Sources 193 (2009) 639–648

Contents lists available at ScienceDirect

Journal of Power Sources

journal homepage: www.elsevier.com/locate/jpowsour

Direct measurement of current density under the land and channel in a PEM fuel cell with serpentine flow fields

Andrew Higier, Hongtan Liu*

Department of Mechanical and Aerospace Engineering, 1251 Memorial Drive, Suite EB 205, University of Miami, Coral Gables, FL 33146, United States

ARTICLE INFO

Article history:
Received 30 January 2009
Received in revised form 25 March 2009
Accepted 26 March 2009
Available online 5 April 2009

Keywords:
PEM
Fuel cell
Current distribution
Current density
Flow field

ABSTRACT

One of the most common types of flow field designs used in proton exchange membrane (PEM) fuel cells is the serpentine flow field. It is used for its simplicity of design, its effectiveness in distributing reactants and its water removal capabilities. The knowledge about where current density is higher, under the land or the channel, is critical for flow field design and optimization. Yet, no direct measurement data are available for serpentine flow fields. In this study a fuel cell with a single channel serpentine flow field is used to separately measure the current density under the land and channel, which is either catalyzed or insulated on the cathode. In this manner, a systematic study is conducted under a wide variety of conditions and a series of comparisons are made between land and channel current density. The results show that under most operating conditions, current density is higher under the land than that under the channel. However, at low voltage, a rapid drop off in current density occurs under the land due to concentration losses. The mechanisms for the direct measurement results and general guidelines for serpentine flow field design and optimizations are provided.

1. Introduction

In an ideal situation the fuel cell components would produce an even current across the entire active area of the fuel cell. However, in a fuel cell with any type of flow field, including the serpentine flow field, the current is not distributed evenly throughout the flow field due to various factors. It is well known that reactant concentration decreases along a flow channel due to reactant consumption and therefore current density tends to decrease along the channel. This problem can be minimized or mitigated by proper flow field designs and by choosing proper operating conditions. For instance, comparison of local current density variations between serpentine and interdigitated flow fields has shown that the latter can produce a more uniform current density distribution across a fuel cell [1]. By properly selecting operating parameters, such as inlet humidification temperature and flow rate, current density along the channel in a serpentine flow field can be controlled [2]. Water flooding can also cause severe non-uniform current density distributions as demonstrated in [3]. Spernjack et al. [4] used a visualization technique to correlate water blocking the flow channels with cell performance. It was determined that the type of GDL used and operating conditions greatly affect the water distribution in the channels and that in turn can negatively affect the performance of the cell.

In order to quantify current variations, various local current density measurement techniques have been developed. Specifically there are three main techniques used to measure local current densities in a fuel cell as described in [5]. The first is a technique where the MEA is broken down into partial MEAs. The second involves creating small sections of MEA or sub-cells throughout the cell. The third involves segmenting the flow field or flow plate itself and mapping the current.

In 1998, Cleghorn et al. [6] used a printed circuit board approach to measure the current density distribution inside a fuel cell. In 2001 Brett et al. [7] used a 'non-intrusive' method for measuring current distribution along a single channel in a PEM fuel cell where a single channel was machined into a printed circuit board. In 2002 Rajalakshmi et al. [8] evaluated the current distribution in a PEM fuel cell using a segmented cell approach. The study determined that pressure drop along the channel is responsible for improper gas distribution and that many of the corners of the channel also have inadequate reactant distribution as well as potential water build-up which causes gas distribution problems. In 2005 Natarajan and Van Nguyen [9] studied the effect of electrode configuration and electronic conductivity on current density distribution using a segmented electrode and corresponding model. The experimental portion of the study consisted of a segmented electrode with a single gas feed channel. In 2005 Sun et al. [3] developed a technique using a specially designed gasket for measuring current distribution in a PEM fuel cell. Later in 2007, Sun et al. [2] used the same measuring gasket technique to study the gas humidification effects and found very different patterns of local

* Corresponding author. Tel.: +1 305 284 2019.
E-mail address: hliu@miami.edu (H. Liu).

0378-7753/$ – see front matter © 2009 Elsevier B.V. All rights reserved.
doi:10.1016/j.jpowsour.2009.03.059

current distributions at different humidification temperatures. In 2007 Brett et al. [10] reported on membrane resistance and current distribution. The study focused on localized current distribution measurements along a single channel.

As described above, all of these studies reported on current distribution in a PEM fuel cell, however, none of them investigate how the current distribution varies laterally across the land and channel. Due to the difficulties of measuring current density laterally under the land and channel, most of the studies done to date utilize mathematical models in order to try and predict the current density under the land and channel.

The early models neglected the electrical resistance of the GDL, catalyst layer and flow plates. The results of these models showed that the area under the land always had a much lower current density (e.g. [11–14]). Natarajan and Van Nguyen [15] showed that the current density under the land was basically zero when the land width is 2 mm or greater.

Later models took into account the lateral resistance of the GDL. In 2004 Meng and Wang [16] developed a model that took into account the lateral resistance of the GDL and found that it played a critical role in current distribution. A CFD model developed by Sivertsen and Djilali in 2005 [17] predicted that the maximum current density actually occurs under the land due to the dominant influence of ohmic losses. Also Lin and Nguyen [18] in 2006 found that the lateral resistance of the GDL plays an important role in current distribution.

Zhou and Liu [19] presented modeling results that incorporates the anisotropic nature of the GDL electrical resistance. The results showed that using realistic through-plane and lateral GDL conductivities, the effect of GDL lateral electrical resistance was not large enough to cause the current density under the land to be higher than that under the channel under any realistic operating conditions.

In 2006 Freunberger et al. [20] used a method for calculating the current density in sections parallel to the flow channels. Their method involved using a number of very thin wires placed in parallel with the channels. The Laplace equation was then used to convert this measurement into a number for current density. Their model domain was a slice perpendicular to the channel direction, composed of the MEA, GDLs and flow field plates on either side. The Laplace equation is then solved for the entire cross-section of the cell perpendicular to the channel direction. The results showed that while operating on air, the current density distribution was fairly constant over the rib and land, though there were some fluctuations with increases at the rib channel interface. As the current density increased the current over the channel increased greatly and the current of the rib sections dropped almost to zero.

Recently, in 2007 Wang and Liu [21], from the same laboratory as this group, used a partially catalyzed membrane for measuring current distribution under the land and channel separately for a parallel flow field. The results showed that under most practical operating conditions, current density under the land is higher than that under the channel. In order to check if such an unexpected result is caused by the additional lateral GDL electrical resistance as stated in some modeling work [16,17], a silver mesh was added in between the GDL and the graphite plate. The results showed that there was no significant change in current density under the channel, thus it showed that lateral resistance of the GDL is not the cause of the higher current under the land area. The most common type of flow field used in PEM fuel cells is the serpentine flow field. The knowledge of where current density is higher, under the land or the channel, is critical for design and optimizations of such flow field. Yet, to date, no direct measurement data are available and the only reported direct lateral current measurements were for parallel flow fields [21]. All the research on lateral current variations for serpentine flow fields was based on mathematical modeling and yet the predicted results are extremely controversial with totally different patterns of current distributions [11–20]. Therefore, the main objective of this study is to separately measure the current density under the land and the channel in order to obtain a definitive answer as to where the current density is higher and to study the effects of various operating parameters.

2. Experimental methodology

In the experiments conducted, the cathode side utilizes a specially designed flow plate with only two channels and one land area as shown in Fig. 1. The channel length is 5.7 cm with a depth of 1 mm. The anode side of the fuel cell is a 50 cm^2 serpentine flow field with both land and channel depth 1 mm; the length of the anode channels is 6.6 cm. The anode channels run horizontally while the cathode channels run vertically. Both anode and cathode flow plates are graphite with machined channels. The graphite flow plates are compressed with two stainless steel endplates and eight tie rods are used to control the cell compression as well as alignment. The current is collected via two gold plated copper collector plates, placed in between the graphite flow plates and the endplates.

The technique used to separately measure the current under the land and channel areas in a PEMFC is similar to that used in [21]. The cathode is chosen for the experiments because, due to the fast kinetics of the half reaction at the anode, the cathode reaction has been found to be the limiting reaction in the PEM fuel cell. In an EIS study done by Springer et al. [22] it was shown that there is a negligible voltage loss and negligible impedance at the anode at all current. In order to isolate the land and channel areas and therefore measure the current density under each one separately, only the area being measured has catalyst. For example, when measuring the current density under the land, only the area of the membrane under the land is a fully catalyzed. Furthermore, a very thin layer of Teflon® is placed in between the gas diffusion layer and the membrane for the area not catalyzed. This design is different from that used in [21], where no insulation between the gas diffusion layer and the catalyst layer was provided. Teflon© insulation aside, the fuel cell used to test in [21] is the same as is used in the current experiments, even the cell compression is maintained the same. This design ensures that the area which is not being studied is completely electrically insulated from the MEA being studied. In addition, because the Teflon layer is the same thickness as the catalyst layer compression is not effected.

Fig. 2(a) and (b) shows a diagram of how the membrane was catalyzed in order to measure current separately under land and channel area. In this manner a wide variety of experiments are carried out which include different operating pressures, flow rates, dewpoints and cathode reactants (air and oxygen).

The membrane used in the fuel cell was Nafion® 117 from Alfa-Aesar. The electrodes for the anode and cathode sides were provided by BCS Fuel Cells. Both the anode and the cathode gas diffusion

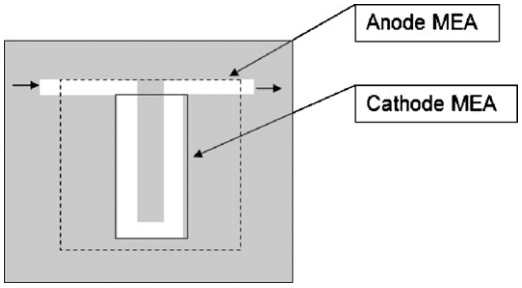

Fig. 1. Schematic (not to scale) of the 2 mm land 2 mm channel single pass serpentine flow field used in the experiments. The white represents the machined channels of the flow field. Also shown are relative sizes of the anode and cathode MEAs.

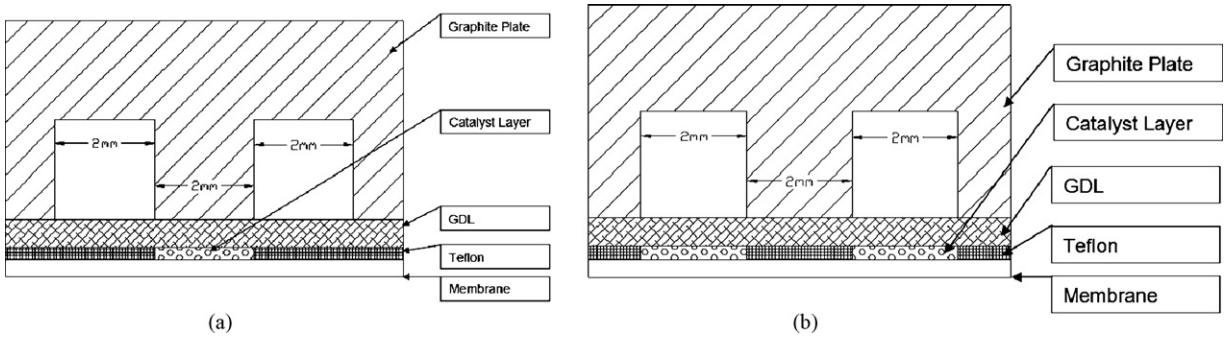

Fig. 2. (a) Cross-section of catalyzed land area. (b) Cross-section of catalyzed channel area.

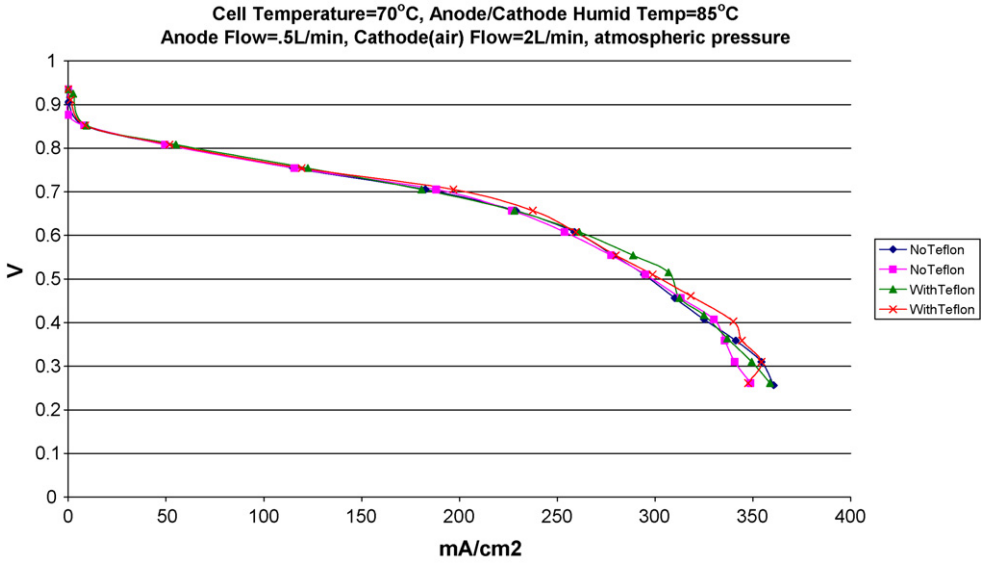

Fig. 3. Graph of Land MEA with and without Teflon© insulation under the channel.

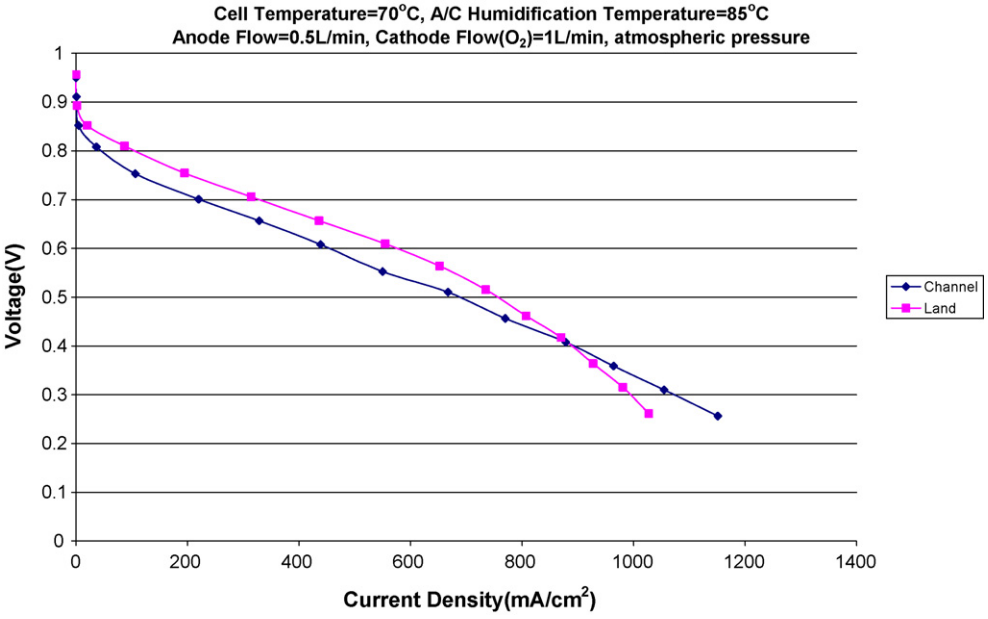

Fig. 4. Comparison of current density under land and channel using oxygen on the cathode.

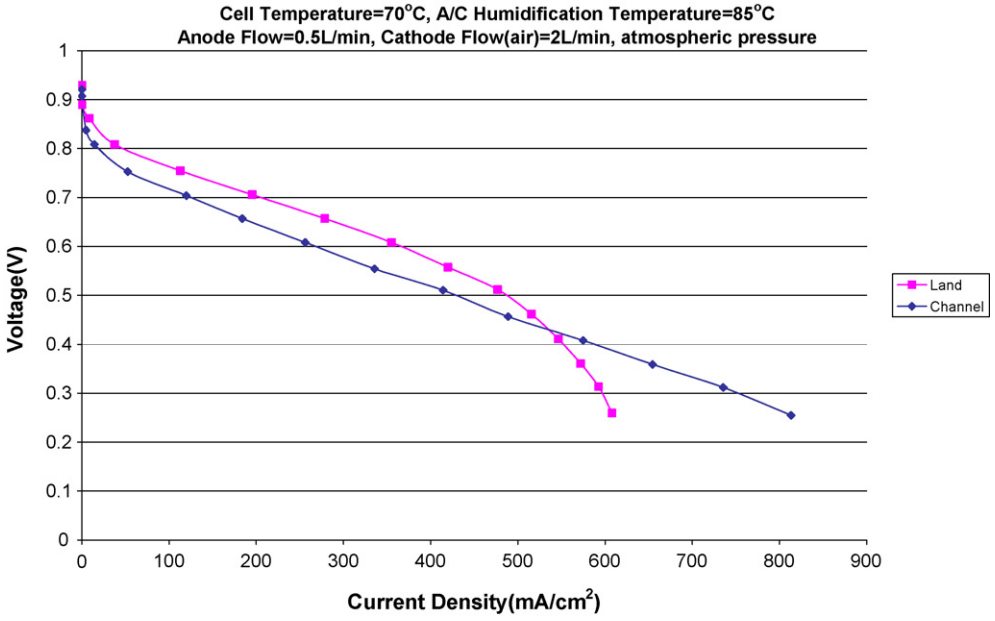

Fig. 5. Comparison of current density under land and channel using air on the cathode.

electrodes (GDL) are carbon cloth with platinum based electrodes. The platinum catalyst loading on both the anode and cathode was 0.4 mg cm^{-2}. The area of the anode electrode was 50 cm^2. The anode was a full size MEA in order to avoid any interference of the anode side in the experiment. The MEAs were assembled and hot-pressed in house.

Prior to conducting the experiments described below, the optimum humidification temperatures were found for this particular MEA and fuel cell. Based on a series of polarization curves as well as electrochemical impedance spectroscopy (EIS) test the cell performed best at anode and cathode humidification temperatures of 85 °C and a fuel cell temperature of 85 °C. In addition, each polarization plot is run three times with a 45 s delay at each point. The voltage is controlled and the current recorded. The results are checked for repeatability and then averaged.

3. Experimental results and discussion

In order to elucidate the differences in performance between the area under the land and the area under the channel it is necessary to compare the results side by side. Making this comparison gives a unique insight into how this type of flow field could be used in specific applications. The first set of experiments performed was to find out if the use of Telfon© has a significant effect on the results, that is, if the previous technique used in [21] can cause significant errors. The results are shown in Fig. 3. It can be seen that there is no significant effect in adding the layer of insulation. Even though this insulation layer is not necessary for measuring current density, throughout all the experiments this insulation layer is used for additional measurements, the results of which will be reported in a separate paper.

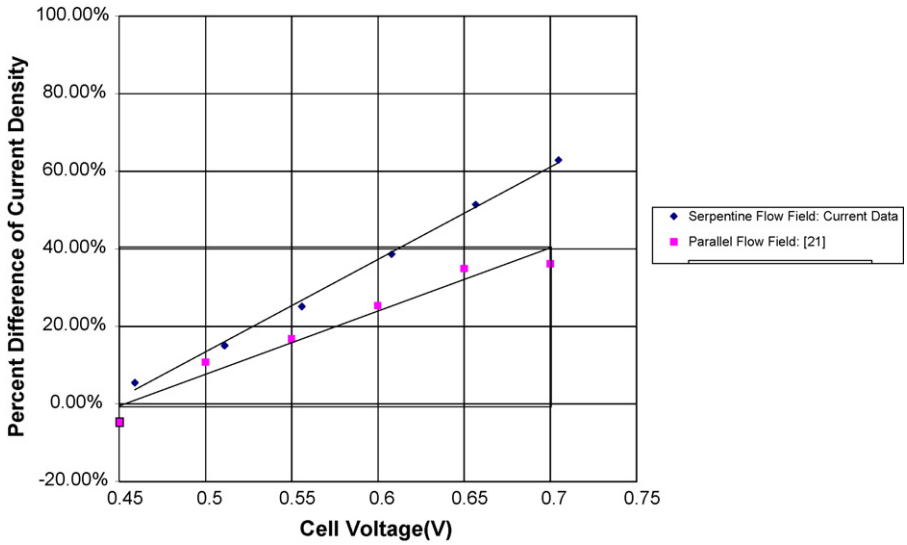

Fig. 6. Comparison of current density increase from land to channel in current experiments and [21].

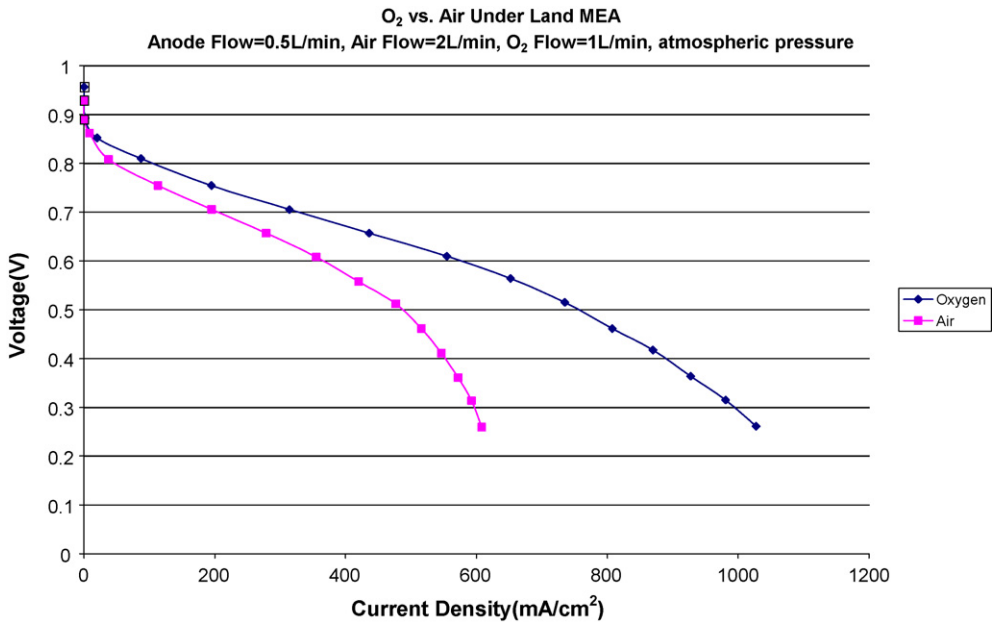

Fig. 7. Comparison of current densities under the land when using either oxygen or air.

3.1. Oxygen and air

Two sets of experiments were conducted using either oxygen or air as the reactant on the cathode side and the results are shown in Figs. 4 and 5. The results definitively show that no matter if air or oxygen is used, current density is higher under the land than under the channel, except at the low cell voltage region. Current density is higher under the land by up to 20% when using oxygen and up to 28% when using air. These trends are the same as those found in [21]. As pointed out above, the trends found in this study for serpentine flow fields are the same as those for parallel flow fields [21]. However, carefully comparing the results, one can find that for serpentine flow fields, the difference in performance between the land and the channel is greater than that found in parallel flow fields. This difference can be attributed to the cross-channel convection underneath the land due to the pressure difference between the channels. In a serpentine flow field, the adjacent channels are hydraulically connected in series, and the downstream channel has a lower pressure. When two channels at different pressure are connected by a porous media, the GDL, convection through the GDL will definitely occur. This convection can significantly increase the reactant concentration under the land area, thus increase the local current density under the land compared to those without this cross-channel convection found in a parallel flow field. Fig. 6 shows an example of the comparisons between the serpentine flow flied (current study) and parallel flow filed [21] in percentage increase in current under the land over that under the channel. It is clear from Fig. 6 that the difference between land and channel performance is significantly higher in a serpentine flow field than in a parallel channel flow field. This trend is observed at a variety of operating parameters.

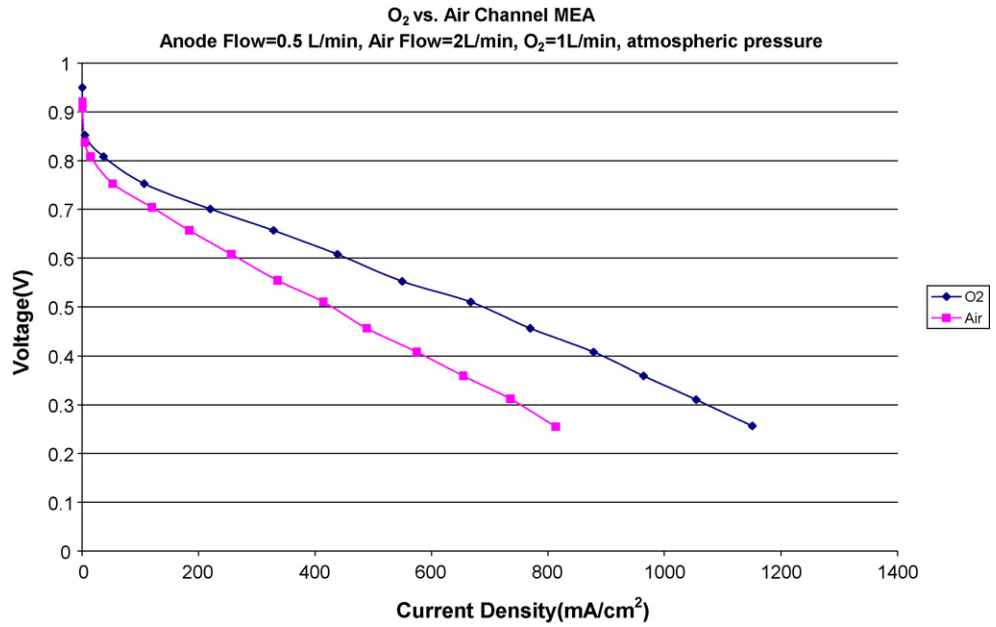

Fig. 8. Comparison of current densities under the channel when using either oxygen or air.

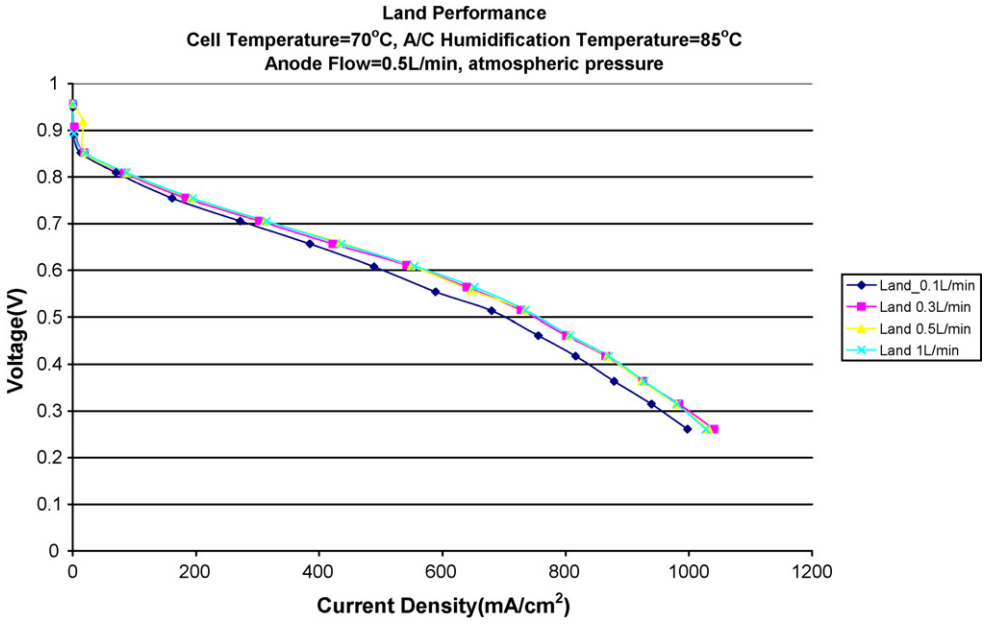

Fig. 9. Effects of oxygen flow rate on current density under the land.

These results unequivocally demonstrate that the increased compression under the land in a fuel cell has a significant effect on the performance. These results also show that current fuel cell models need significant improvements in order to correctly predict local current density distributions.

As can be seen from Figs. 4 and 5, the main difference between the results using air and oxygen is the concentration losses under the land. In the case of pure oxygen, the concentration losses, that is, the losses due to lack of oxygen, are small under the land. It can be seen that when air is used the drop off due to concentration losses not only occurs at higher voltage, but that the drop off is more rapid. This drop off, both in the case of oxygen and air, is due to the concentration losses which in turn are caused by lower effective porosity under the land due to the higher compression of the GDL as well as the increased travel length of the reactant. This corresponds well to a study done by Nitta et al. [23] in 2006, which found that the GDL intrusion into the channel is significant and that the compression that the GDL experiences under the land is far greater that what the GDL experiences under the channel. This increased compression under the land is simultaneously the cause of the lower electrical resistance and the higher mass transport losses.

In order to further clarify the differences between land and channel using oxygen and air it is helpful to plot the results of land and channel separately. Fig. 7 shows the performance under the land and the difference in performance when oxygen and air are used. It is clear that not only is the performance lower using air, but the

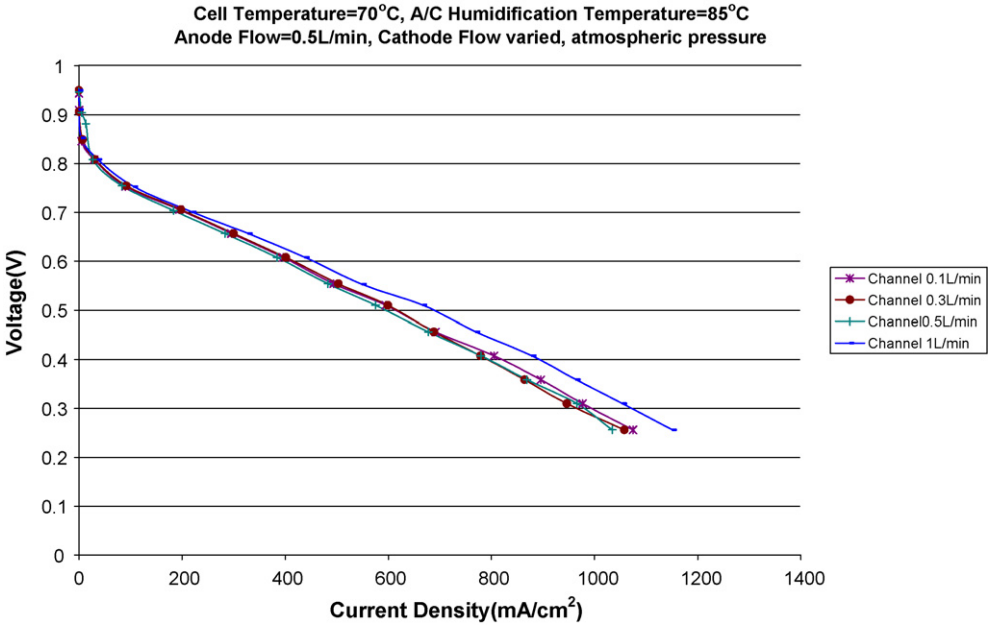

Fig. 10. Effects of oxygen flow rate on current density under the channel.

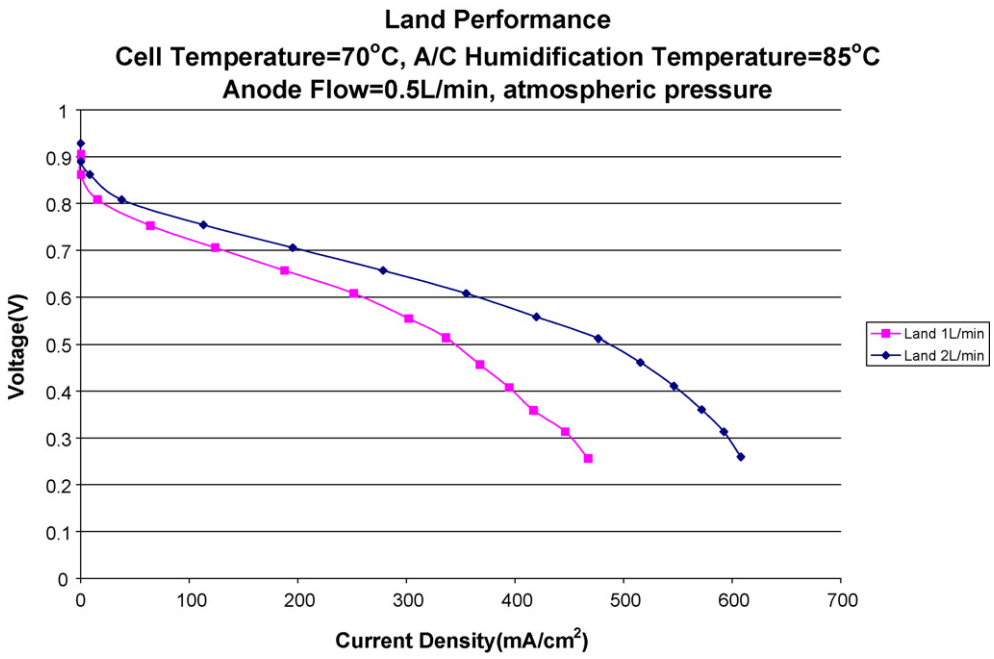

Fig. 11. Effect of air flow rates on current density under the land.

concentration losses are far more significant as indicated by the rapid drop off in performance.

Fig. 8 shows the performance under the channel and the difference in performance when oxygen and air are used. It is clear from comparing Figs. 7 and 8 that the performance under the channel is not significantly affected by concentration losses, while the performance under the land is.

3.2. Different flow rates

Different flow rates were tested using either air or oxygen on the cathode side in order to investigate the effect of flow rate on current density under the land and channel. Fig. 9 shows the effects of oxygen flow rate on performance under the land and it is clear that, above 0.1 L min^{-1} the effect of flow rate on performance is minimal, indicating that any further increase in flow rate beyond 0.1 L min^{-1} cannot increase the oxygen concentration at the reaction sites.

Fig. 10 shows the results on the effects of oxygen flow rate on current density under the channel. Again it can be seen that the effects of oxygen flow rate are minimal, however, here a slightly different trend is observed; only at high flow rates of 1 L min^{-1} is any increase in performance seen. Also, comparing Figs. 9 and 10 it can be noted that there is a slight downward sloping trend at low voltages under the land whereas no downward turn occurs at all under the channel. This difference is as expected since under the channel, oxygen is very accessible and no concentration losses are observed.

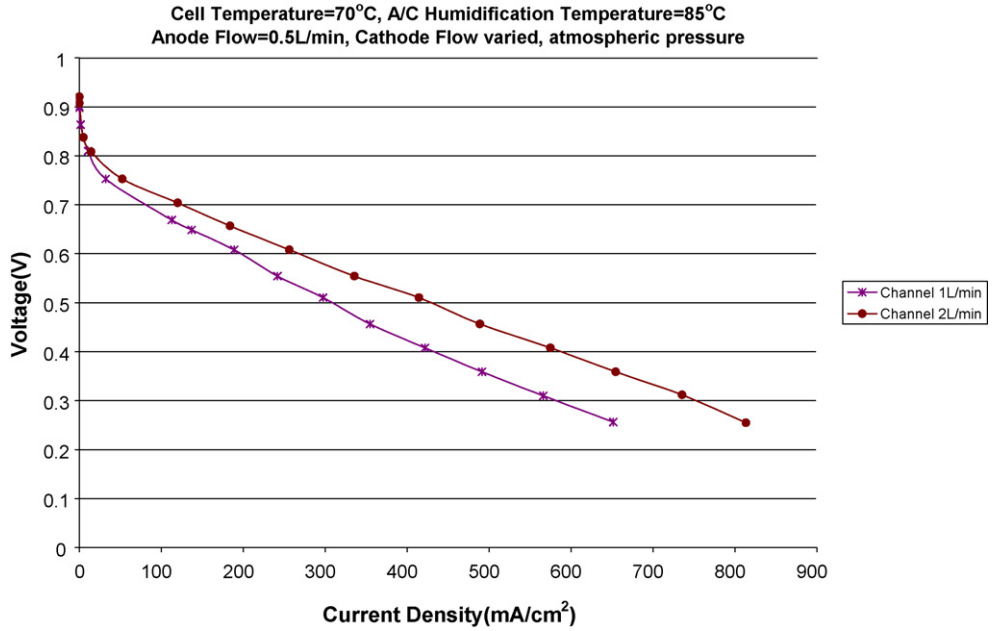

Fig. 12. Effect of air flow rates on current density under the channel.

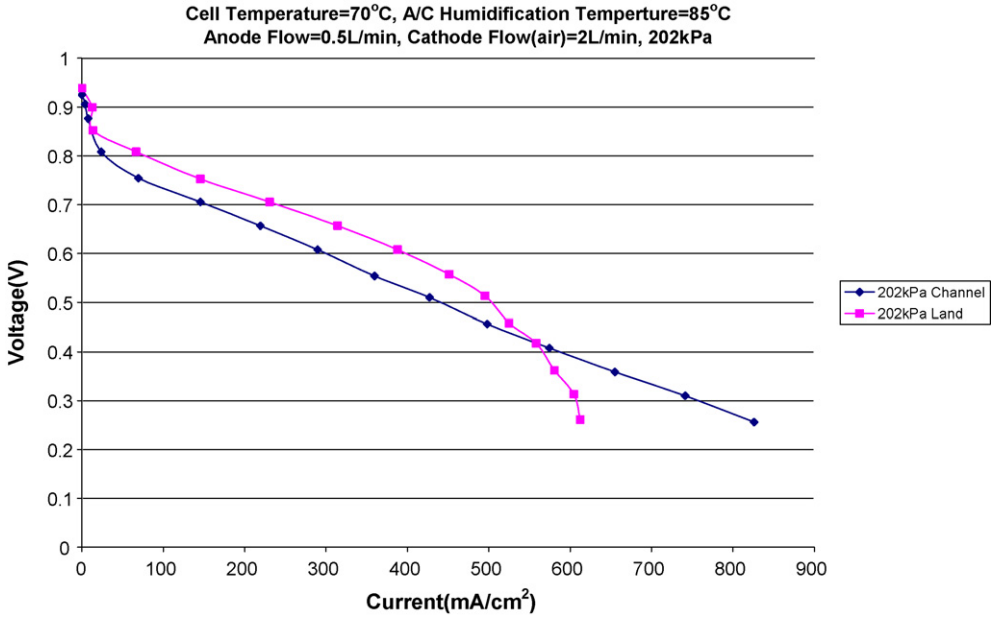

Fig. 13. Comparison of current density under the land and channel at 202 kPa pressure.

Fig. 11 shows the results of air flow rate on the current density under the land. It is clear from Fig. 11 that the air flow rate has a significant effect on performance under the land. In fact, below 1 L min^{-1} the performance becomes very unstable and erratic; therefore only two different flow rates were presented. Fig. 12 shows the effect of different air flow rates under the channel. Again there is a significant difference in performance between 2 L min^{-1} and 1 L min^{-1} air flow rates but no concentration losses can be observed.

3.3. Different pressures

A series of experiments are conducted in order to investigate the effect of pressure on performance under the land and channel. All pressures reported are absolute pressure. Fig. 13 shows the comparison of current density under the land and the channel at 202 kPa and it can be seen that the result for the 202 kPa are similar to that for 101 kPa. That is, the performance under the land is higher in the high voltage region of the polarization curve but drops drastically in the low voltage region.

Fig. 14 shows the comparison of current density between the land and channel at 303 kPa. At 303 kPa the mass transport losses under the land are lower, and the difference in current density between the land and the channel is greater. Comparing Figs. 14–16 it is clear that the difference in current density between the land and the channel increases as pressure increases at high cell voltage. For instance, at 0.75 V, the current density under the land is twice high as that under the channel. It is also interesting to note that the crossing point, where the land and channel current densities are equal, move toward higher current density as pressure increases.

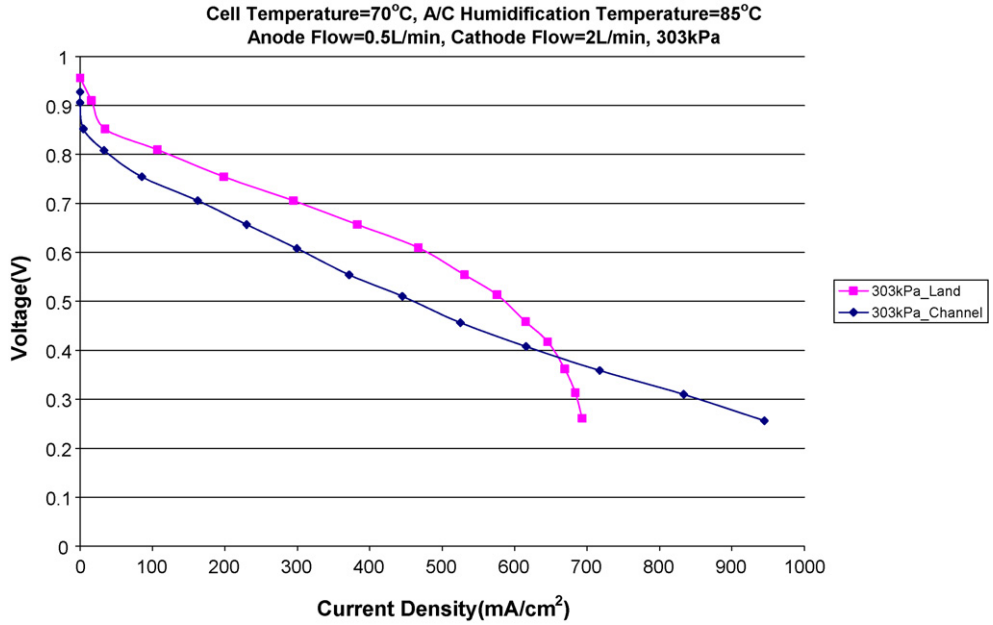

Fig. 14. Comparison of current density under the land and channel at 303 kPa pressure.

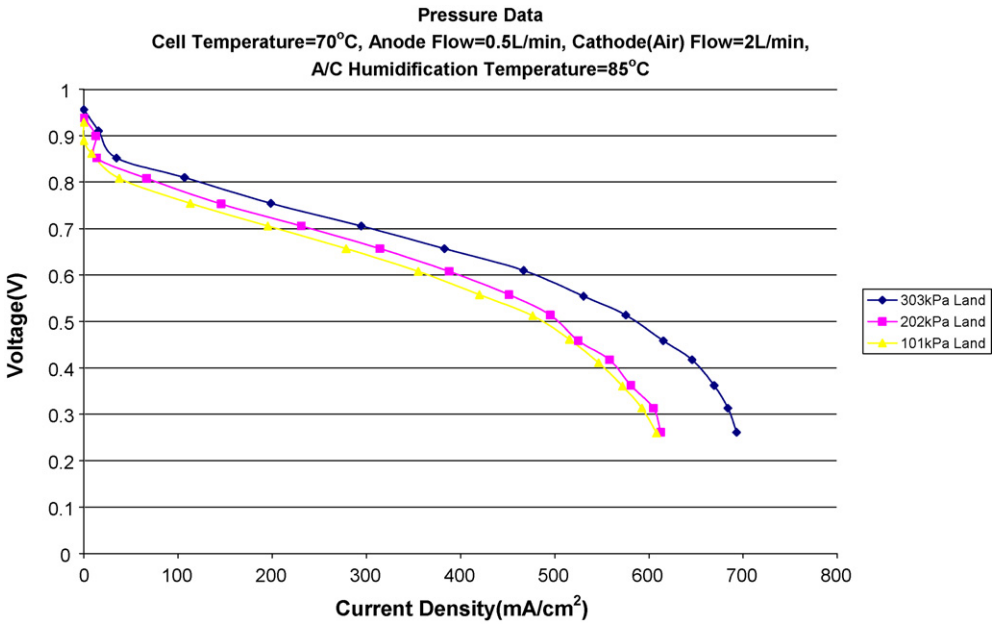

Fig. 15. Comparison of current densities under the land at various pressures.

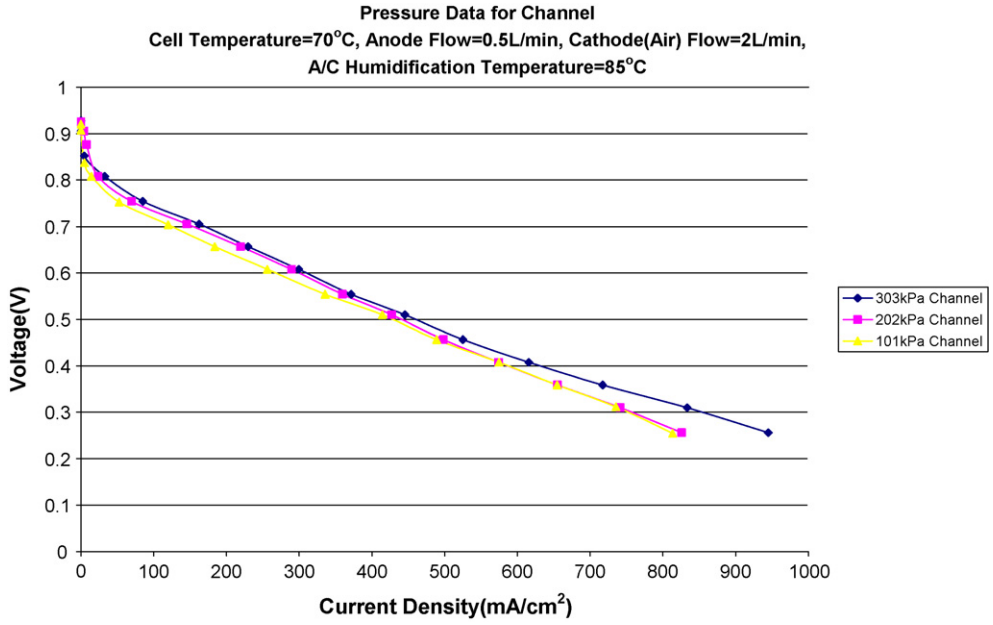

Fig. 16. Comparison of current densities under the channel at various pressures.

This is due to the fact that as pressure increases, mass transfer rate increases and the detrimental effect of the additional mass transfer resistance under the land decreases. It is obvious from these results that, for a fuel cell designed for high pressure operations, the width of the land could be larger than those designed for low pressure operations.

To further show the different effects of pressure on the current densities under the land and the channel, Figs. 15 and 16 are presented. Fig. 15 shows the current densities under the land at different pressures and Fig. 16 shows those under the channel. From Fig. 15 it can be clearly seen that current density under the land increases with the increase in pressure, though the sharp drop in current density due to concentration losses is always present. In contrast, it is clear from Fig. 16 that the differences in current density under the channel at different pressures are not significant and no sharp drop in current density due to concentration losses can be observed.

4. Conclusion

A technique, created in house, is used to separately measure the current density under the land and channel in a single pass serpentine flow field with a 2 mm wide channel and a 2 mm wide land area. The cathode side of the MEA was catalyzed either over the land or the channel area depending on the desired area to be measured. In this manner a series of experiments were carried out in order to

determine the current density over the land and the channel separately. Based on the experimental results, the following conclusions can be made.

- Under most operating conditions, current density of a fuel cell with serpentine flow fields is higher under the land than under the channel in most practical operating cell voltages.
- Cross-channel convection underneath the land due to pressure difference is significant in enhancing cell performance under the land.
- The concentration losses are always significant under the land in high current density region regardless of operating pressure, cathode flow rates or if air or oxygen is used.
- In the range of flow rate used in this study, no significant concentration losses can be observed under the channel even when air was used at atmospheric pressure.
- Flow fields design, specifically the widths of the channel and the land, must be customized for a particular application to achieve optimal performance and the optimal design is highly dependent on the operating voltage and other operating conditions.

References

[1] G.S. Zhang, L. Guo, B. Ma, H. Liu, J. Power Sources, in press.
[2] H. Sun, G. Zhang, L.-J. Guo, S. Dehua, H. Liu, J. Power Sources 168 (2007) 400–407.
[3] H. Sun, G. Zhang, L.-J. Guo, H. Liu, J. Power Sources 158 (2006) 326–332.
[4] D. Spernjak, A.K. Prasad, S.G. Advani, J. Power Sources 170 (2007) 334–344.
[5] J. Stumper, S.A. Campbell, D.P. Wilkinson, M.C. Johnson, M. Davis, Electrochem. Acta 43 (24) (1998) 3773–3783.
[6] S.J.C. Cleghorn, C.R. Derouin, M.S. Wilson, S. Gottesfeld, J. Appl. Electrochem. 28 (1998) 663–672.
[7] D.J.L. Brett, S. Atkins, N.P. Brandon, V. Vesovic, N. Vasileiadas, A.R. Kucernak, Electrochem. Commun. 2 (2001) 628–632.
[8] N. Rajalakshmi, M. Raja, K.S. Dhathathreyan, J. Power Sources 112 (2002) 331–336.
[9] D. Natarajan, T. Van Nguyen, J. Power Sources 135 (2004) 95–109.
[10] D.J.L. Brett, S. Atkins, N.P. Brandon, N. Vasileiadis, V. Vesovic, A.R. Kucernak, J. Power Sources 172 (2007) 2–13.
[11] T. Zhou, H. Liu, Int. J. Trans. Phenomena 3 (2001) 177.
[12] T. Berning, D.M. Lu, N. Djilali, J. Power Sources 106 (2002) 284, 437.
[13] U. Sukkee, C.Y. Wang, J. Power Sources 125 (2004) 40, 438.
[14] D. Natarajan, T.V. Ngyuen, J. Electrochem. Soc. 148 (2001) A1324.
[15] D. Natarajan, T. Van Nguyen, AIChE J. 51 (9) (2005).
[16] H. Meng, C.Y. Wang, J. Electrochem. Soc. 151 (2004) A358, 440.
[17] B.R. Sivertsen, N. Djilali, J. Power Sources 141 (2005) 65, 441.
[18] G. Lin, T.V. Nguyen, J. Electrochem. Soc. 153 (2006) A372.
[19] T. Zhou, H. Liu, J. Power Sources 161 (2006) 444.
[20] S.A. Freunberger, M. Reum, J. Evertz, A. Wokaun, F.N. Büchi, J. Electrochem. Soc. 153 (11) (2006) A2158–A2165.
[21] L. Wang, H. Liu, J. Power Sources 180 (2008) 365–372.
[22] T.E. Springer, T.A. Zawodzinski, M.S. Wilson, S. Gottesfeld, J. Electrochem. Soc. 143 (2) (1996).
[23] I. Nitta, T. Hottinen, O. Himanen, M. Mikkola, J. Power Sources 171 (2007) 26–36.